

Healthy and Diabetic Primary Human Osteoblasts Exhibit Varying Gene Expression Profiles in High and Low Glucose Environments on 3D-Printed Titanium Surfaces

Nicholas Allen¹, Bijan Abar², Julian Buendia Burbano, Richard Michael Danilkowicz³, Lindsey Johnson, Alexandra Hunter Aitchison⁴, Mark Montgomery, Samuel Bruce Adams

¹Duke University School of Medicine, ²Duke, ³Duke University Medical Center, ⁴Hospital For Special Surgery

INTRODUCTION:

3D printing is becoming an increasingly popular manufacturing technique for orthopaedic implants used in spine, trauma, and extremity surgeries. Because the technique of 3D printing fuses titanium powder, there is an inherent natural surface roughness that is quite different from traditionally milled implants and could be beneficial for osseointegration. In foot and ankle surgery, 3D printed implants are being used to treat bone defects from diabetic Charcot collapse. However, diabetes is known to negatively affect bone metabolism leading to nonunion and decreased osseointegration to traditionally manufactured orthopaedic implants. There are no studies examining how diabetic osteoblasts respond to 3D printed surfaces. The purpose of this study was to characterize osteogenic gene expression profiles of both healthy and diabetic primary human osteoblasts cultured on a medical grade 3D-printed titanium surface in the presence of high and low glucose environments. Furthermore, to characterize the phenotypic changes that arise in the presence of an *in vitro* osteoblast-titanium surface environment, our study sought to investigate the variations in cell morphology, matrix deposition, and mineralization that play a predominant role osteoblast adhesion and integration into 3D fabricated titanium implants currently being utilized in orthopaedics.

METHODS: Healthy and diabetic primary osteoblasts were isolated from discarded healthy and Charcot patient bone fragments, expanded to confluence in osteogenic expansion medium (α-mem, 10% fetal bovine serum, 1% anti/anti) using standard tissue culture technique and pooled to generate respective healthy and diabetic osteoblast populations. 3D printed discs were produced using medical grade titanium alloy powder (Ti6Al4V) with an average diameter of 35 μm, conforming with chemistry appropriate for implanted medical device per ASTM F3001. Healthy or diabetic osteoblasts were seeded at 10e4 cells/disc in a 48 well plate and allowed to adhere for 4 hours. The expansion media was aspirated and the healthy and diabetic-laden discs were cultured in complete osteogenic medium (DMEM, 10% FBS, 1% anti/anti, 10 mM β-glycerolphosphate, 50 μg/mL ascorbic acid) containing high (4.5 g/L D-glucose) or low glucose (1 g/L D-Glucose) concentrations. Conditioned media was collected at days 3, 7, 14, and 28 for quantification of alkaline phosphatase (ALP). At days 14 and 28 discs were fixed in 10% neutral buffered formalin for scanning electron microscopy (SEM) or alizarin red staining. Real-time polymerase chain reactions (RT-qPCR) were conducted at days 1 and 28 using primers to quantify osteoblast mRNA expression of *Bglap* (osteocalcin), *Col1a1*, and *Bmp7*.

RESULTS: SEM images depicted in figure 1 reflect the cellular morphology and extracellular matrix (ECM) deposition of healthy and diabetic osteoblasts cultured in high and low glucose at days 14 and 28. At day 14, a dense and organized ECM can be observed in the healthy group, regardless of glucose concentration. Conversely, in the diabetic osteoblast group, much of the titanium surface (round blobs) is still visible and a less confluent deposition of ECM can be observed. At day 28, both healthy and diabetic osteoblast groups appear to maintain a dense and confluent ECM regardless of media glucose content. Alizerin red staining (figure 2a) reflecting the extent of mineralization at days 14 and 28 indicated a trend in increased mineralization in healthy osteoblast groups, though not significant. Furthermore, a trend in increased mineralization of healthy osteoblasts cultured in high glucose medium is present, whereas, a slight decreasing trend can be observed in the diabetic osteoblast groups cultured in the presence of higher glucose concentrations. Alkaline phosphatase activity (figure 2b) quantified from the conditioned medium collected at days 3, 7, 14, and 21 all exhibit an increasing behavior with the exception of healthy osteoblasts cultured in high glucose medium. While these values were found to be insignificant, the ALP activity of both diabetic and healthy osteoblasts cultured in either high or low glucose seems to remain conserved. RT-qPCR results revealed an increased expression of *Bglap* (osteocalcin) in groups cultured in high glucose medium (figure 2c). While these results were not significant, an observable increase in osteocalcin gene expression can be observed in healthy osteoblasts. *Col1a1* expression was significantly elevated in healthy osteoblasts cultured in high glucose medium in comparison to baseline and low glucose results (figure 2d). Additionally, healthy osteoblast *Col1a1* expression was significantly higher than that of the diabetic osteoblasts cultured in high glucose media. *Bmp7* expression at day 28 was significantly higher in healthy osteoblasts cultured in high glucose medium in comparison to its baseline value (figure 2e). Furthermore, a general trend in increased healthy osteoblast *Bmp7* expression can be observed in both high and low glucose environments.

DISCUSSION AND CONCLUSION: Healthy and diabetic primary human osteoblasts exhibit notable variations in osteogenic gene expression, mineralization, and matrix deposition that warrants attention. Here we further characterize the impact that a high or low glucose environment plays on primary healthy and diabetic osteoblasts in the presence of a 3D-printed titanium surface.

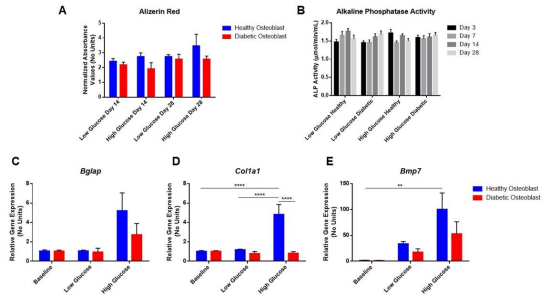


Figure 2. (a) Alizarin red mineralization quantification. (b) ALP activity in conditioned medium. (c) *Bglap* relative gene expression. (d) *Col1a1* relative gene expression. (e) *Bmp7* relative gene expression.

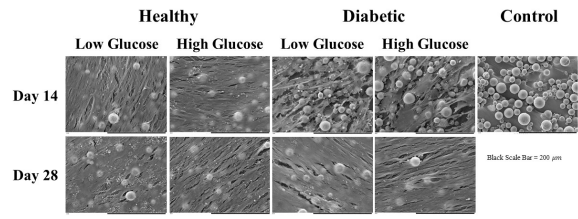


Figure 1. SEM images of experimental groups at days 14 and 28.